Czech Technical University in Prague
Faculty of Nuclear Sciences and Physical Engineering
Department of Physics

RESEARCH WORK

Simulation of DNA damages induced by incorporated ^{125}I

Praha, 2005 **Hedvika Toncrova**

Contents

List of Figures

List of Tables

Chapter 1

Introduction

It has already been a long time since radiobiologists have found a high toxicity of the Auger emitting radionuclide ^{125}I being incorporated into deoxyribonucleic acid (DNA). Nowadays, this radionuclide is of widespread use in nuclear medicine and still an subject of extensive investigation. Scientists are able to attach the ^{125}I atom to so a called targeting agent that finds an exact sequence in the DNA and then incorporates the Iodine atom here. There the Iodine decays and causes hard damages, which can even lead to cell death. This process is currently being used e.g. in some types of a cancer radiotherapy.

Once bounded in the DNA, the ^{125}I ultimately decays. The decay is followed by a shower of low-energy Auger electrons. These electrons interact at first with atoms of DNA itself and this causes damage of the biomolecule. Further, the radiation interacts with water molecules, radiolytic species are produced and this causes additional lesions to the DNA. Parallel to these processes, a product of the decay - metastable, multiply ionized ^{125m}Te is being neutralized which also has a significant toxic effect.

The radiation action has often been experimentally and theoretically studied and another useful feature has been observed: from a measurement of DNA fragments left after the decay it is possible to determine some particular DNA conformations - e.g. triplexes [1], that cannot be otherwise observed with classical experimental methods.

One of the aims of this work is to build a well working model that could be used to model decay of Iodine incorporated in the DNA and to compare the results with performed experiments. This model can then serve to test possible molecular structures of studied DNA. From the comparison of calculated and measured data (probability of strand breaking along the DNA base sequence) we get information of

how the tested molecular structure corresponds to the real one. An actual version of the model is presented and tested on a well known structure for which a lot of experimental as well as theoretical results are available.

I have already mentioned the significant role played by the neutralization effect. Unfortunately much less information is available about this effect than about the direct radiation effect. The second aim of this work is to clarify the importance of the neutralization effect and introduce it correctly into the model.

To build such a model is one of the ways possible to achieve a deeper understanding of the neutralization effect. In experiments it is not possible to avoid the neutralization of the Tellurium's ion and thus estimate its importance. In a simulation one can easily deduce an approximate extent of the damage caused by all the individual effects. The easiest way is to simulate all the steps without the neutralization and then compare it with experimental data that tells us how much and what kind of damage is caused by the neutralization itself.

Due to the stochastic character of the I^{125} decay a huge number of pathways exist for how the atom can de-excite, and emitted particles further interact. Thus the Monte Carlo (MC) technique is an appropriate tool for simulation of the whole process.

The other possibility is to study directly the neutralization i.e. the charge transfer in DNA. This area of research has recently developed quickly because of number of possible applications e.g. in medicine or nanotechnology.

In this work I'm trying to approach the problem from both sides. At first, I build a model of the radiation action using a MC method. Details of the model and its results are given and then compared to experimental findings. In the second part of the study, the theory of charge transfer is described and a model is found that could possibly be applied to the structure used in the first part.

Chapter 2

^{125}I decay and its radiation action

2.1 ^{125}I decay theory

^{125}I decays in two steps [2]. At first the electron capture (EC) occurs. The nucleus captures an inner-shell orbital electron, typically from a K-shell. The nucleus decays to metastable a ^{125m}Te with an excitation energy of 35.4 keV. The energy may be released by different processes will be explained in a subsection 2.1. The processes mainly involves emission of electrons and photons. Each released electron increases the positive charge on the daughter atom by 1. In average 13 electrons are emitted during this so called first Auger cascade. This is finished in 10^{-16}s to 10^{-15}s.

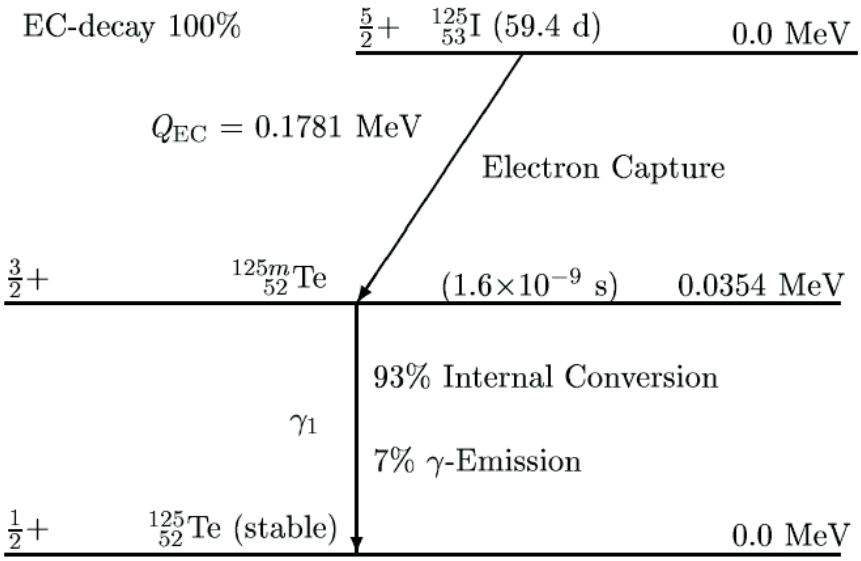

Figure 2.1: Decay scheme of ^{125}I. Taken from [2].

Obviously the Tellurium atom is then in a multiple ionized state. The decay scheme is sketched on Fig.2.1.

The lifetime of ^{125m}Te is 10^{-9}s and it is assumed that in condensed phase, the time is sufficient for the positive charge to be neutralized by electrons from the surrounding molecules. Afterwards the ^{125m}Te decays by γ emission. In 93% of the cases the γ ray is absorbed by an inner shell electron which is ejected as a conversion electron. In these cases the vacancy has to be again filled what gives rise to a second Auger cascade. In condensed phase the outer shells are full and thus the number of Auger electrons emitted is considerably higher than for an isolated atom (15 and 21 electrons respectively). The ^{125}I incorporated in DNA is considered to be in a condensed phase. Electrons for the neutralization are extracted and transferred from the DNA molecule itself as well as from surrounding water molecules.

Vacancy Cascade Transitions

The transitions during a vacancy cascade are classified into three following categories [3]:

1. *Radiative transition.* The initial vacancy is filled by an electron from a higher shell and the gained energy is carried away by a photon. Its energy is determined by the difference between the binding energies of the affected shells. This process doesn't cause any increase in the charge of the atom. The vacancy is moved to a higher shell.

2. *Auger (AUG) transition.* This process is competitive to radiation transitions. The vacancy is filled from a higher principal shell, but the energy is released by emission of another electron. A kinetic energy of the electron is again determined by the difference between the binding energies of the affected shells. During Auger transition the charge of the atom is increased by +1.

3. *Coster-Kronig (CK) transition.* This process is almost identical to Auger transition. Only the electron filling the vacancy comes from a different subshell of the same principal shell, in which the vacancy lies. In general, when energetically possible, the Coster-Kronig transitions have higher probability than Auger transitions.

These three processes can be accompanied by additional vacancy-creating phenomena:

- *Shake-off electron emission.* When a vacancy is created - irrelevant of the responsible mechanism - the entire electron cloud readjust to the new state and a shake-off electron may leave the atom.

- *Double-Auger electron emission.* Two Auger electrons are ejected instead of only one. The double-Auger transition have lower intensities relative to the corresponding normal Auger transitions.

2.2 Experimental measurements of DNA damage caused by incorporated ^{125}I

Damages arising from an Iodine decay have been extensively experimentally studied. The studies were performed on many different structures - on a mammalian cellular DNA, on plasmids, or on synthetic oligonucleotides. A good review of the experiments performed can be found in [2]. For this work we are especially interested in experiments performed on the 41 base-pair long oligonucleotide. There is especially a group of Lochachevsky and Martin that has been working with this structure for a long time (see [4], [5] or [6]). In the section 3.3 the results of our calculations are compared with their data so the next few lines are devoted to a description of their experiments [4].

The base sequence of DNA duplex is specified in the Fig.3.4. Samples of this oligonucleotide were labelled with ^{32}P at either the $5'$ or $3'$ end of either the ^{125}I-containing (so-called top) or opposite (bottom) strand. The ^{32}P-end labelled fragments produced by ^{125}I decays were separated on denaturing polyacrylamide gels, and the quantities of oligonucleotides of different size was determined. If a DNA strand contained more than one break, only the fragment produced by the break nearest to the ^{32}P was registered, as it is shown on the scheme 2.2.

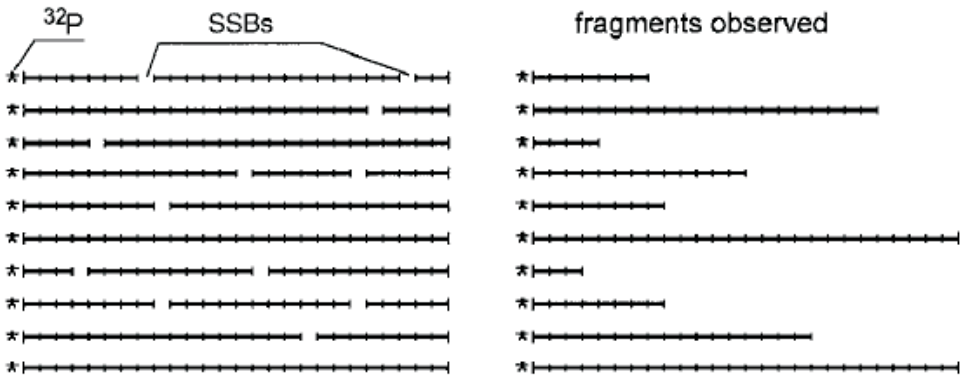

Figure 2.2: The relationship between the real breakage pattern (the left panel) and the observed DNA fragments (the right panel). Only fragments produced by breaks nearest to the ^{32}P label were observed [7].

The fragment size distributions and distribution of single-strand break probabilities as a function of distance from the ^{125}I were presented. To shortly sum up their results, the average yield of single-strand breaks per ^{125}I decay was 3.3 in the top strand and 1.3 in the bottom strand. Each ^{125}I decay event produced a break in the top strand, and a breakage of the bottom strand occurs in 75–80% of the events. Thus a double strand break was produced by ^{125}I decay with a probability of approximately 0.8. The detailed results of the experiments, i.e. graphs of normalized fragment size distributions and probabilities of breakage are shown in the section 3.3 with a direct comparison to our calculated results.

Chapter 3

Simulation of DNA damage caused by incorporated ^{125}I

3.1 Previous studies

Already many authors have tried to model what happens in DNA after the incorporated Iodine decay. A basic building block for all of them was the model of the ^{125}I decay in a condensed phase.

The first attempt to calculate the number and energy distribution of electrons and photons emitted during the disintegration of ^{125}I was performed by Charlton and Booz [8]. They assumed for condensed phase that during the pause between EC and internal conversion (IC) all vacancies created by EC are filled i.e. the complete neutralization. Charlton *et al.* tried to refine their results and presented it in [3]. Anyway their results were not very precise and thus the new method for the Auger cascade simulation was developed by the same group in 1987 [9]. Recently Pomplun utilized experimental data, adapted their program and got results in a very good agreement with the experimental findings [7]. His results have been used as an input for present work.

In the Pomplun's program the following steps were taken. At first the subshell, where the electron capture occurs was chosen randomly according to normalized photon cross sections or to capture and internal conversion probabilities. It was mostly the K-shell, with relative frequency higher then 80% [9]. Starting from this vacancy, the transitions were selected from a list of energetically possible processes according to their probabilities. The radiative as well as Auger and Coster-Kronig and even shake-off and double Auger transitions were considered. All these transition

probabilities are known just for singly ionized atoms, but were modified according to the actual number of electrons available in the shells involved in the particular transition. Next, the new status of the atom was evaluated i.e. the distribution of electrons and vacancies in each subshell was determined. The total energy of this individual atomic state was calculated. The difference in the energy between the initial state (before the transition) and the final one (after the transition) was equated to the kinetic energy of the electron or photon emitted during the transition. This procedure was repeated until all vacancies were localized in the outer shells and no further transition was energetically possible. It was assumed that sufficient amounts of electrons are present in DNA, hence the complete neutralization takes place during the pause between the two Auger cascades. The same procedure was performed by the program after the neutralization. The details of the whole MC simulation can be found in [9, 7]. Yields and energies of emissions in the ^{125}I decay in a condensed phase are listed in the Table 3.1 and have been taken from [7]. The meaning of the notation: CE-K is internal conversion electron from a K-shell. AUG-KLL is an Auger electron emission from a L-shell that occurs when the vacancy in the K-shell is filled by an orbital electron from the L-shell. The energy is directly transferred to the emitted Auger electron. X and Y stays for any shell higher than L-shell. Similarly CK-LLX is an emission of electron during the Coster-Kronig transition in L-shell.

Transition	Yield/decay	Mean energy [keV]
CE-K	8.03E-01	3.64E+00
CE-L_1	9.69E-02	3.05E+01
CE-L_2	7.61E-03	3.09E+01
CE-L_3	1.93E-03	3.11E+01
CE-M_1	1.65E-02	3.45E+01
CE-M_2	3.21E-03	3.46E+01
CE-M_3	8.80E-04	3.47E+01
CE-N_1	3.90E-03	3.53E+01
CE-N_2	8.10E-04	3.53E+01
AUG-KLL	1.33E-01	2.25E+01
AUG-KLX	5.80E-02	2.64E+01
AUG-KXY	5.48E-03	3.02E+01
CK-LLX	2.67E-01	1.85E-01
AUG-LMM	1.25E+00	3.04E+00
AUG-LMX	3.44E-01	3.67E+00
AUG-LXY	2.21E-02	4.29E+00
CK-MMX	1.49E+00	9.42E-02
AUG-MXY	3.31E+00	4.05E-01
CK-NNX	3.33E+00	3.16E-02
AUG-NXY	8.12E+00	1.61E-02

Table 3.1: Transition yields and mean Auger, Coster-Kronig and conversion electron energies for ^{125}I.

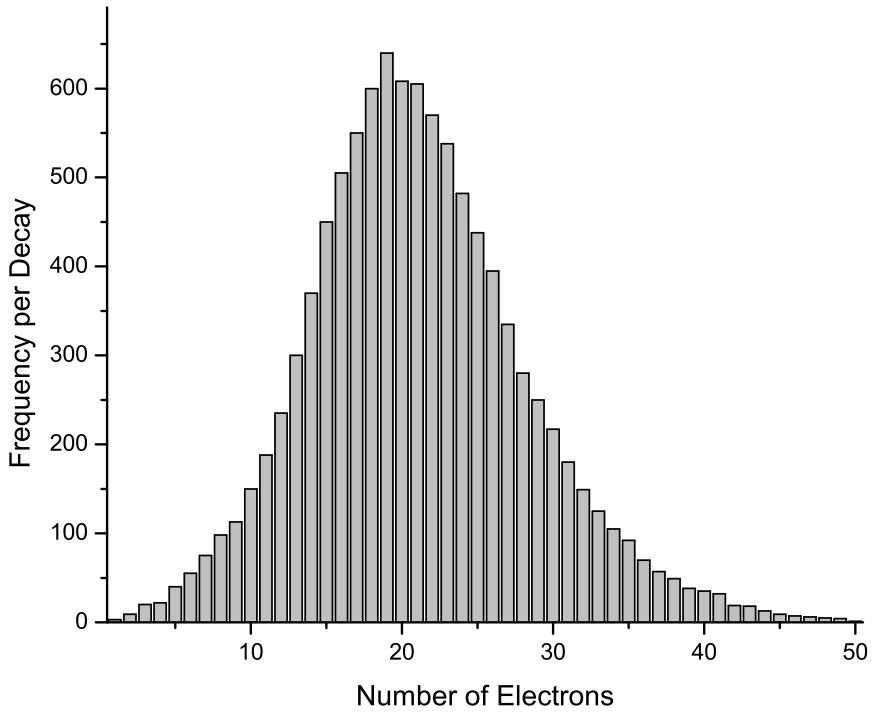

Figure 3.1: Frequency distribution of the number of emitted electrons for 'condensed phase'. According to [7]

In 1986, Charlton used his simple code for the ^{125}I decay and made a first attempt to calculate the consequences of ^{125}I decaying in DNA. In 1987, Pomplun *et al.* [9] published the first data of his Monte Carlo simulation. In 1991, Pomplun [10] developed a new DNA target model, based on coordinates of individual atoms. This enabled the distinction between direct and indirect electron hits. Recently the same author published a paper [11] where he discussed the neutralization effect. He concluded that it has an non-negligible effect and needs to be incorporated into molecular simulations.

In 1994, Terrissol published results that he obtained from a simulation on a more complex DNA model. The same year Pomplun and Terrissol [12] also investigated the behavior of chemical radicals produced in the water shell after the ^{125}I decay.

In 1996, Nikjoo *et al.* published their first results obtained from their model. After a few years of developing the model they applied it in 2000 [13] on a triplex-forming oligonucleotide and compared the results to a classical duplex-forming oligonucleotide. Also in this paper they have for the first time presented the idea of using

Auger electrons as a probing agent for the study of structures of nucleic acids.

Since 1998 a group of Friedland, Paretzke *et al.* have been working on their model. They have been presenting their work continuously since then e.g. in [14], [15], [16]. The most complex review of their work was published in 2002 by their cooperator Weibo Li in his PhD thesis [2]. Some of their results are shown later in the section 3.3.

3.2 Our model

Our simulation is performed in several steps (details of each step will be given later)

1. Number of emitted electrons and their energies are randomly chosen according to the data presented in the section 3.1.

2. Electron tracks in the liquid water are modelled using a computer program `TRIOL`. Interaction coordinates and deposited energy for each interaction event are found.

3. Each electron track is randomly rotated in space with its origin located at the spatial coordinates of the Iodine atom.

4. The track coordinates are superimposed with DNA atoms' coordinates. A hit is encountered, when the interaction occurs within a Van der Waals radius of some DNA atom.

5. The biological effect of energy deposition is analyzed. The hits leading to DNA strand breaks are recorded.

3.2.1 ^{125}I decay

At first, a number of emitted electrons for a particular decay is chosen using a frequency distribution in a condensed phase according to Fig.3.1. This distribution has been calculated by Pomlun [7]. The particular electrons, with their energy are then selected according to the yields presented in Table.3.1. This is done using random numbers. The selection is of course very rough, because not all combinations of electrons are allowed. In reality the electrons are emitted during successive transitions and thus limiting conditions of energy transitions need to be introduced to the program.

The electron energy spectra are shown and compared with the data used by Li [2] in the Fig.3.2.

The difference in energy spectra is obvious. While according to Li the peaks are separated from each other, in our spectra we have the continuum. As I have already said, this is because energetically not all the transitions are allowed. Also the peaks for very low energies are too high in our simulation. These inaccuracies caused errors in our results, that will be described later.

3.2.2 The electron tracks

In the section 3.2.1 it is described how the ^{125}I decay is simulated and thus how the emitted electrons and their energies are chosen. To evaluate their biological effect we need to let them interact with the DNA molecule and its surroundings.

Radiation interacts with matter in different processes and their probabilities are expressed as cross sections. Living cells are mostly composed of water (it constitutes approx. 70% of the cells weight [17]) and also each DNA molecule is in a natural environment that is heavily hydrated. We see that in an ideal case the cross sections for DNA atoms as well as for liquid water would be needed for the simulation. Unfortunately information about cross sections for DNA are limited, but they are expected to be very similar to the cross sections of water. Thus the particle tracks (i.e. the spatial distribution of the primary interactions) were modelled in liquid water.

The particle tracks are simulated using a program called TRIOL, developed by Bigildeev and Michalik [18]. It is a Monte Carlo program based on previously developed program called TRION for a water vapor [19]. Two representatives of electron tracks, one high energy and the second low energy are presented in the Fig. 3.3.

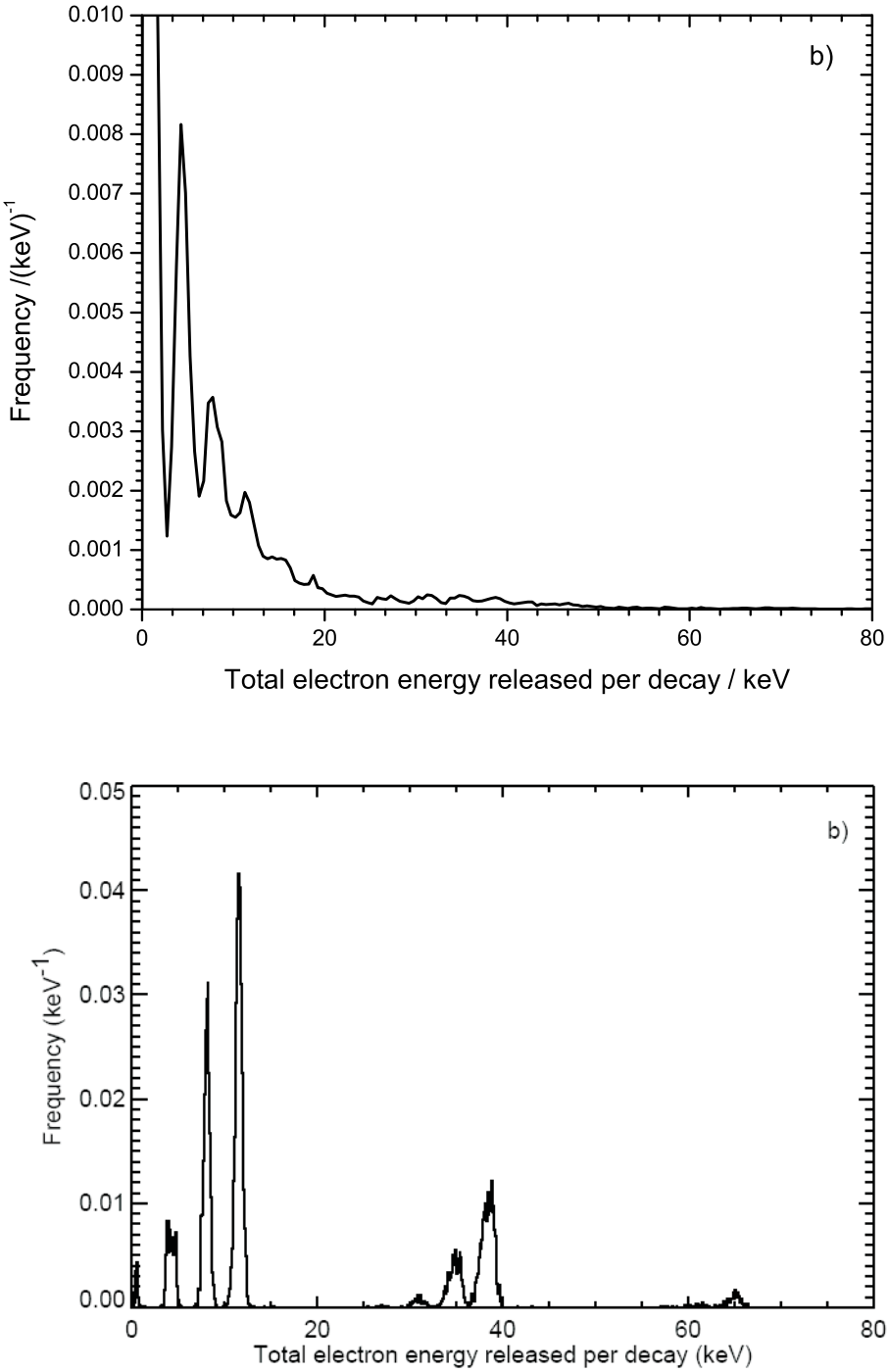

Figure 3.2: The frequency of total electron energy released per decay as used a) in our simulation b) in Li's simulation [2].

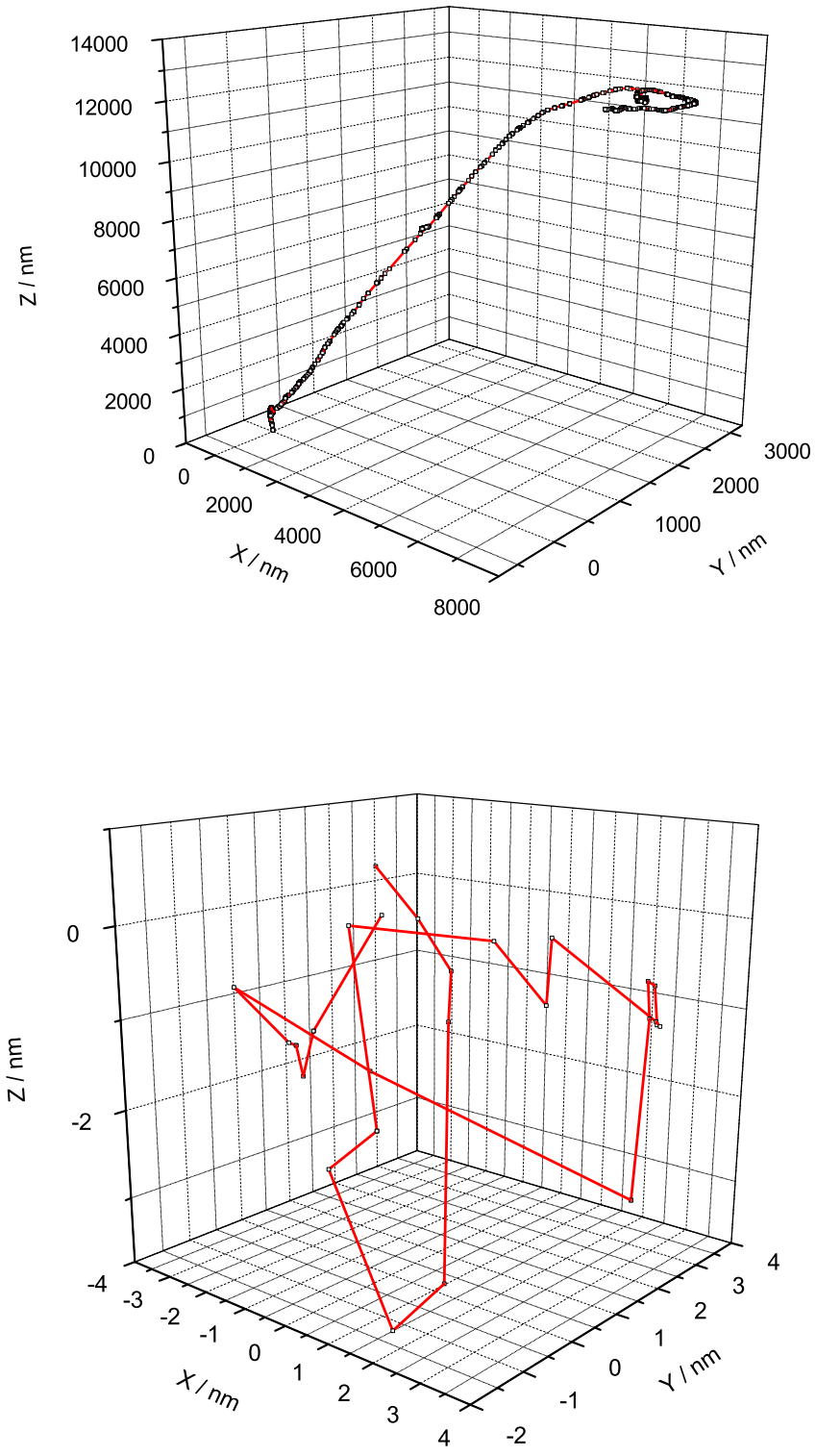

Figure 3.3: Upper panel - a track of a high energetic CE-N1 (for notation see section 3.1) with initial energy 35.3 keV. Lower panel - a track of a low energetic CK-MMX electron with initial energy 0.094 keV, both modelled using a computer program TRIOL. The trajectories are depicted with the red line, locations of energy deposition with black dots. Note the scales of the figures.

3.2.3 DNA structure

A DNA strand is a macromolecular chain of building units called nucleotides. Each nucleotide is further composed from 3 different moieties - base, sugar and phosphate moiety. The phosphate and sugar are the same for all the nucleotides, the bases however are of four types: adenine (A), guanine (G), cytosine (C) and thymine (T).

The DNA double helix is formed when two single strands combine to form an extended array of A-T and G-C base pairs. The helix is held together by hydrogen bonding between the complementary bases and stabilized by their stacking interactions. The structurally well-defined DNA π stack may represent a unique medium for electron transfer. This is important during the neutralization phase as we shall see in the section **??**.

The DNA structure model used is a synthetic 41-mer oligonucleotide, containing the ^{125}I atom that replaces a hydrogen on C5 of the middle cytosine base. This is a typical target for which many experiments ([20], [4], [5]) as well as theoretical calculations ([2], [14], [15]) have been performed.

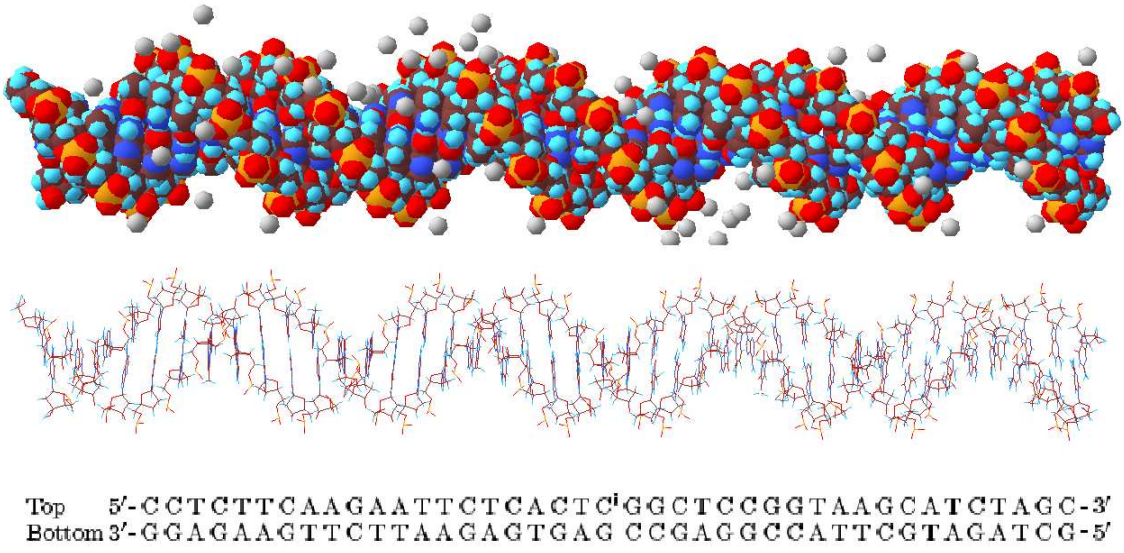

Figure 3.4: DNA structure model of a synthetic 41-mer oligonucleotide. On two upper panels is shown a molecular structure created by AMBER 7, on the lowest panel the sequence of nucleobases. The notation of DNA bases: adenine (A), guanine (G), cytosine (C), and thymine (T), C^i shows the cytosine with the incorporated ^{125}I.

As was mentioned above a DNA molecule in its natural environment is heavily hydrated. A DNA surface is in general negatively charged and thus it polarizes

Atom	VdW Radius / nm
H	0.12
C	0.17
O	0.152
N	0.155
P	0.18

Table 3.2: Van der Waals radii of atoms used in present study.

the surrounding water molecules that form a quite rigid water shell around it. The thickness of this water shell is approximately 0.5 - 0.6 nm.

The molecular structure of 41-mer oligonucleotide, including the water shell was created using a program called `AMBER 7` [21]. As a starting point, a part of `AMBER` called `Nucgen` was used to generate cartesian coordinates of DNA atoms in standard conformation. This structure was then later energy minimized using another subprogram called `Sander`. The result is shown in Fig. 3.4.

3.2.4 Superposition of electron tracks on DNA and analysis of a biological effect

While superimposing the interaction events with the DNA coordinates several assumptions are taken then concerning a hit occurrence. The events that do not fall into a cylinder of diameter 3 nm, enclosing the DNA double helix, are automatically redirected to a chemical module (which will be a next step in the model development), i.e. they are not counted to direct or "quasi-direct" radiation action. Further on, an atom closest to the event is selected i.e. either DNA atom or water-shell atom. For the DNA atoms, the hit occurs when the interaction event falls into one Van der Waals radius of the DNA atom. The Van der Waals radii used are listed in Table 3.2. The hit means that an event, e.g. ionization or excitation happens and deposits its energy inside DNA atom. Where and how much of the energy is deposited in the DNA molecule is important whilst calculating the damage to the molecule.

The energy deposition inside the molecule can lead to chemical bond breakages or to other damage of the complicated structure of DNA molecule. The biological consequences are most serious for single and double strand breaks. Single strand break (SSB) is a simple break of the backbone of one polynucleotide strand. If two breaks occur on the opposite strands in within a distance of 10 - 15 base pairs we speak about a double strand break (DSB). Thus in the simulation we are most

interested in the SSBs.

A SSB is assumed to occur in DNA if a local energy deposition exceeds the ionization threshold of liquid water, i.e. 10.79 eV [2]. If the energy is lower, a simple hit is encountered. The biological consequences of such hits can be found e.g. in [22], [2] and will not be discussed here.

Events occurring inside the water shell, not more than 0.6 nm far from a closest DNA atom [1], are classified into three categories:

1. *Water molecules attached to a phosphate group.* 60% of these events are taken as "quasi-direct" hits, i.e. they are considered as if they would appear directly on the phosphate group. 40% are to be further processed in the chemistry module [2].

2. *The molecules attached to sugar-group atoms.* All these events will be directly transferred to the chemistry module.

3. *The events appearing in molecules attached to bases* are supposed to result in base damage.

The events that occur inside the water shell, but more than 0.6 nm far from the DNA are redirected to the chemical module. This model for consequences of energy deposition was taken from Li [2].

3.3 Results and discussions

We ran the simulation for 50000 independent decays. This number of decays was statistically tested and for this number the convergence of results was reached. The DNA target used was presented in section 3.2.3. In the actual state of the model we only observe direct and quasi-direct hits. They represent the nonscavangeable part of the experiment without the neutralization effect and can thus be easily compared with experimental findings. The comparison to results obtained by Li, described in section 3.1, is also presented.

The break probability distributions of our simulation are plotted for the top and bottom strands in the Fig.3.5. The distribution is also plotted separately for the hits arising from the direct and the quasi direct effects in figures 3.6 and 3.7. The fragment size distribution calculated by our program is shown in Fig. 3.8 and 3.9.

[1] i.e. there are not more than 2 water molecules between the event and the DNA molecule

The comparison with experimental data is made on the fragment size distribution for both ^{32}P-labelled 5′-end and 3′-end. The experiment was performed by Lobachevsky and Martin [4], [5] in phosphate buffer (PB) solution with high scavenging capacity, which means that only strand breaks arising from direct and quasi-direct hits together with neutralization effect have contributed. The fragment distribution is shown in the Fig.3.11. These results were also transformed to a break probability distribution and are shown with direct comparison with simulation data of Li [2] in the Fig.3.10.

The simulation should show less strand breaks than the experiment, because the neutralization effect is not counted. Martin and Lobachevsky obtained in average 3.3 single-strand breaks per decay in the top strand and 1.3 in the bottom strand, whereas we obtained 2.7 and 2.4 SSBs per decay in the top and bottom strand respectively. This means that we got too many strand breaks, because the neutralization effect is usually assigned a contribution of 30-50% .. reference!!!! . Also the profile of the graph is different, especially the two peaks appearing in our simulation at the distance of 10 bases from the decaying ^{125}I. After an analysis of our code we concluded that the problem lays in the Auger cascade simulation. As I have mentioned, the way we chose the electrons to be emitted after the decay is unprecise. This causes, that we get too many high energy electrons that cause the far-away breaks (more than 5-6 base pairs far). The two additional peaks around the bases 11 and 31 come from the geometrical conformation of DNA. The DNA molecule is a double helix and thus the base one turn far is closer in the space than the bases closer in the same chain.

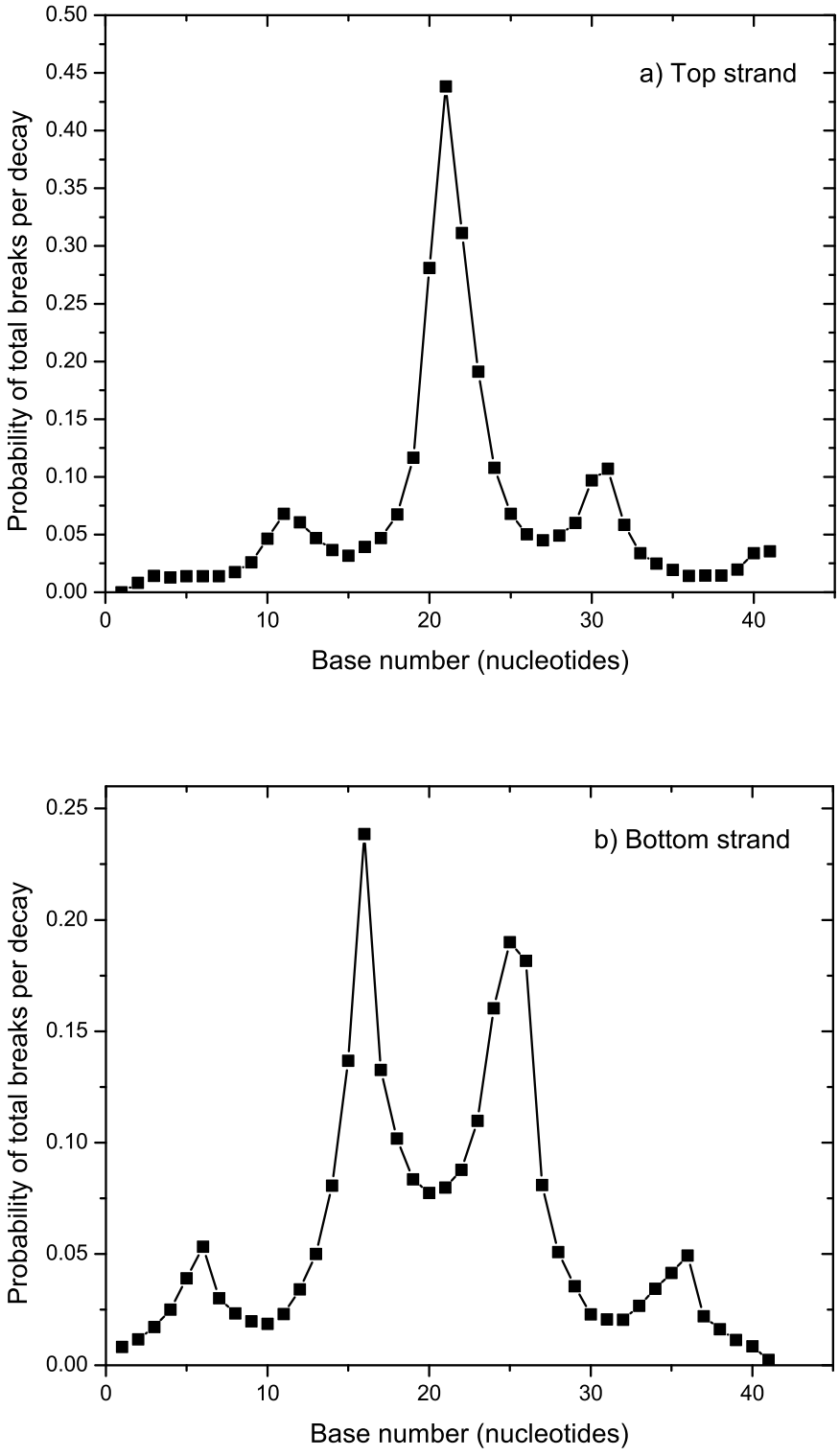

Figure 3.5: The calculated probability of strand breaks arising from direct and quasi direct hits per ^{125}I decay in the 41-mer oligonucleotide in the top strand (panel a) and in the bottom strand (panel b).

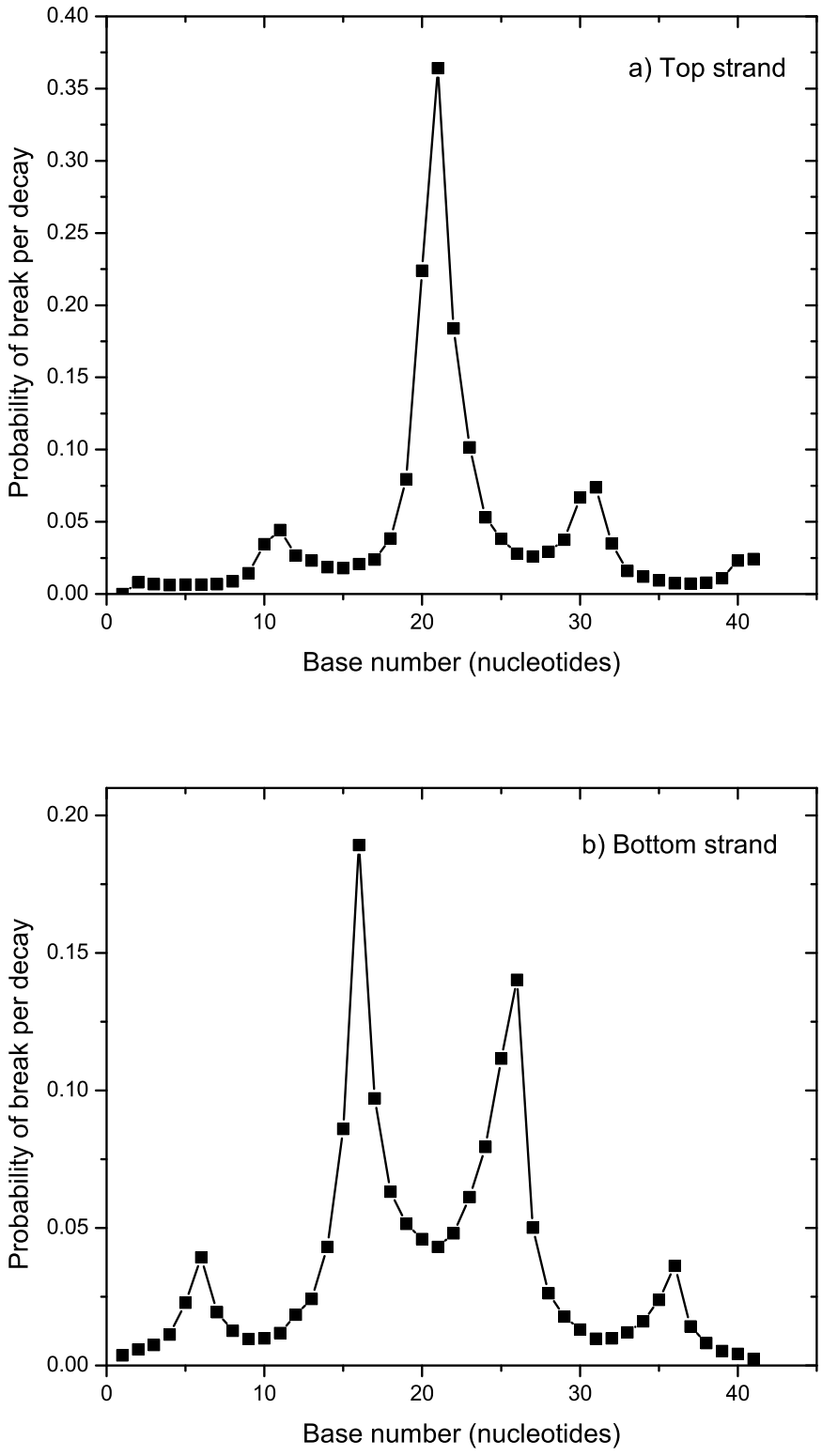

Figure 3.6: The calculated probability of strand breaks arising only from direct hits per ^{125}I decay in 41-mer oligonucleotide in the top strand (panel a) and in the bottom strand (panel b).

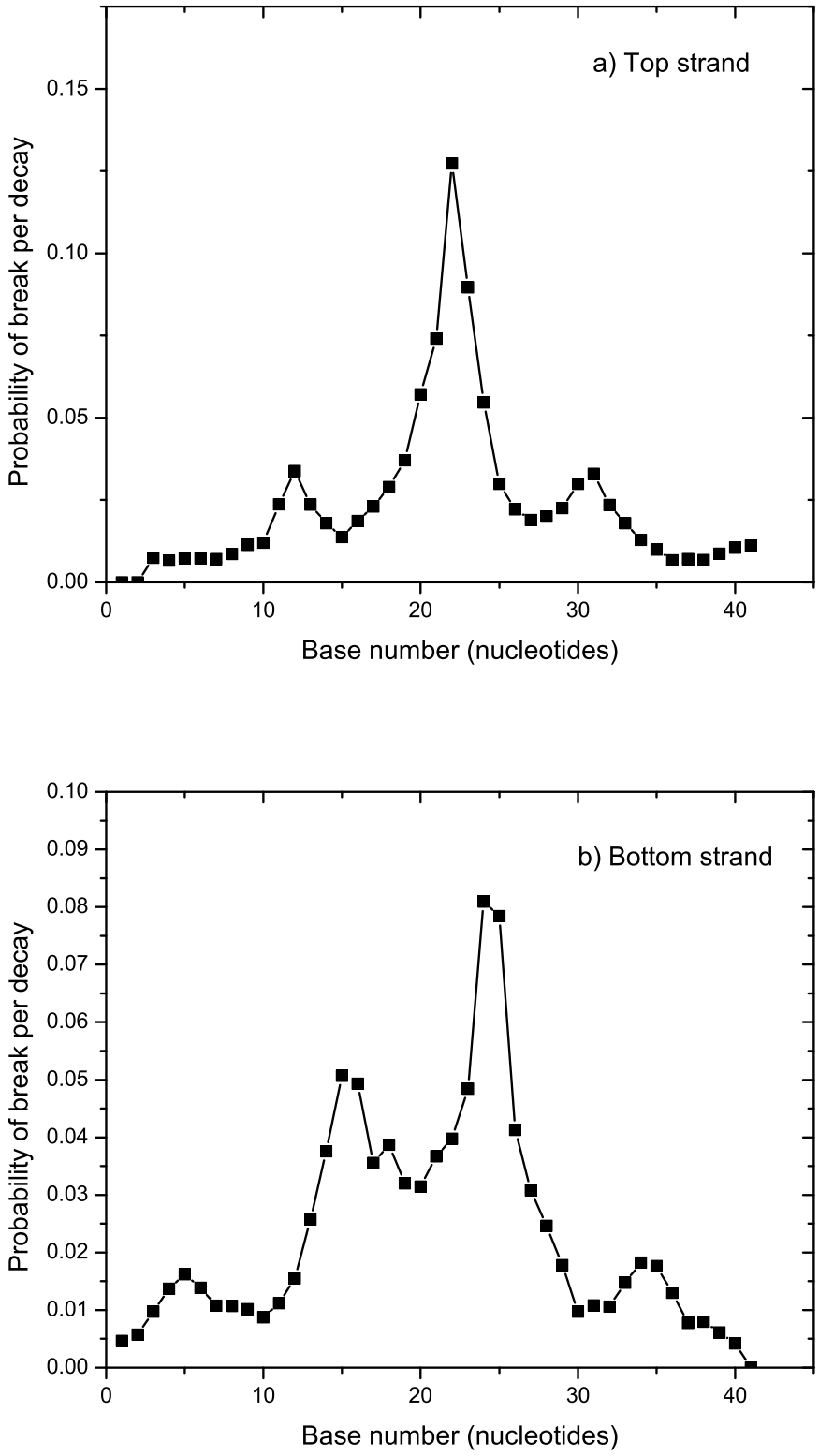

Figure 3.7: The calculated probability of strand breaks arising only from quasi-direct hits per ^{125}I decay in 41-mer oligonucleotide in the top strand (panel a) and in the bottom strand (panel b).

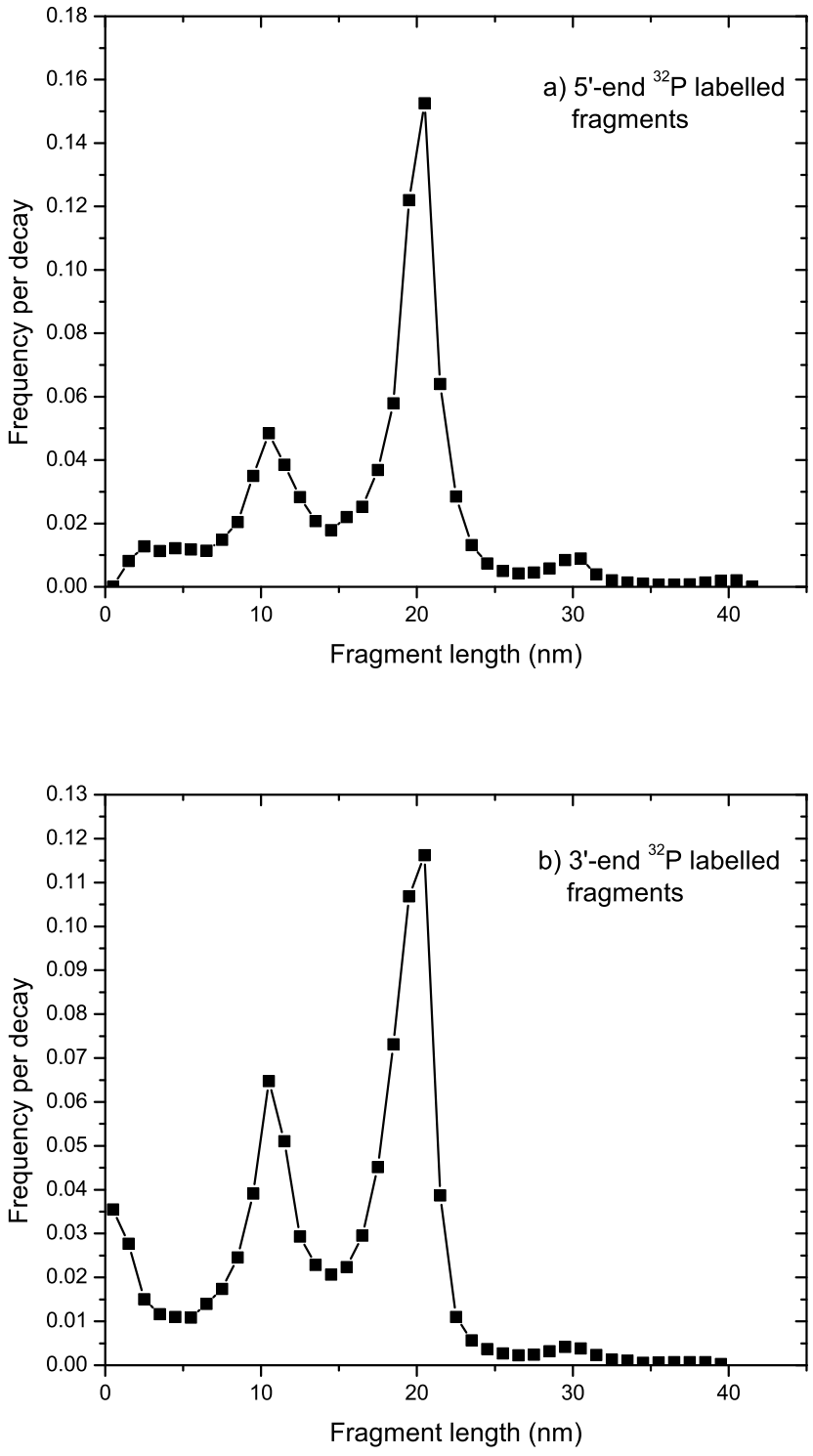

Figure 3.8: The calculated fragment size distribution resulting from breakage in the top strand. Panel a: 5′-end ^{32}P-labelled fragments; panel b: 3′-end ^{32}P-labelled fragments.

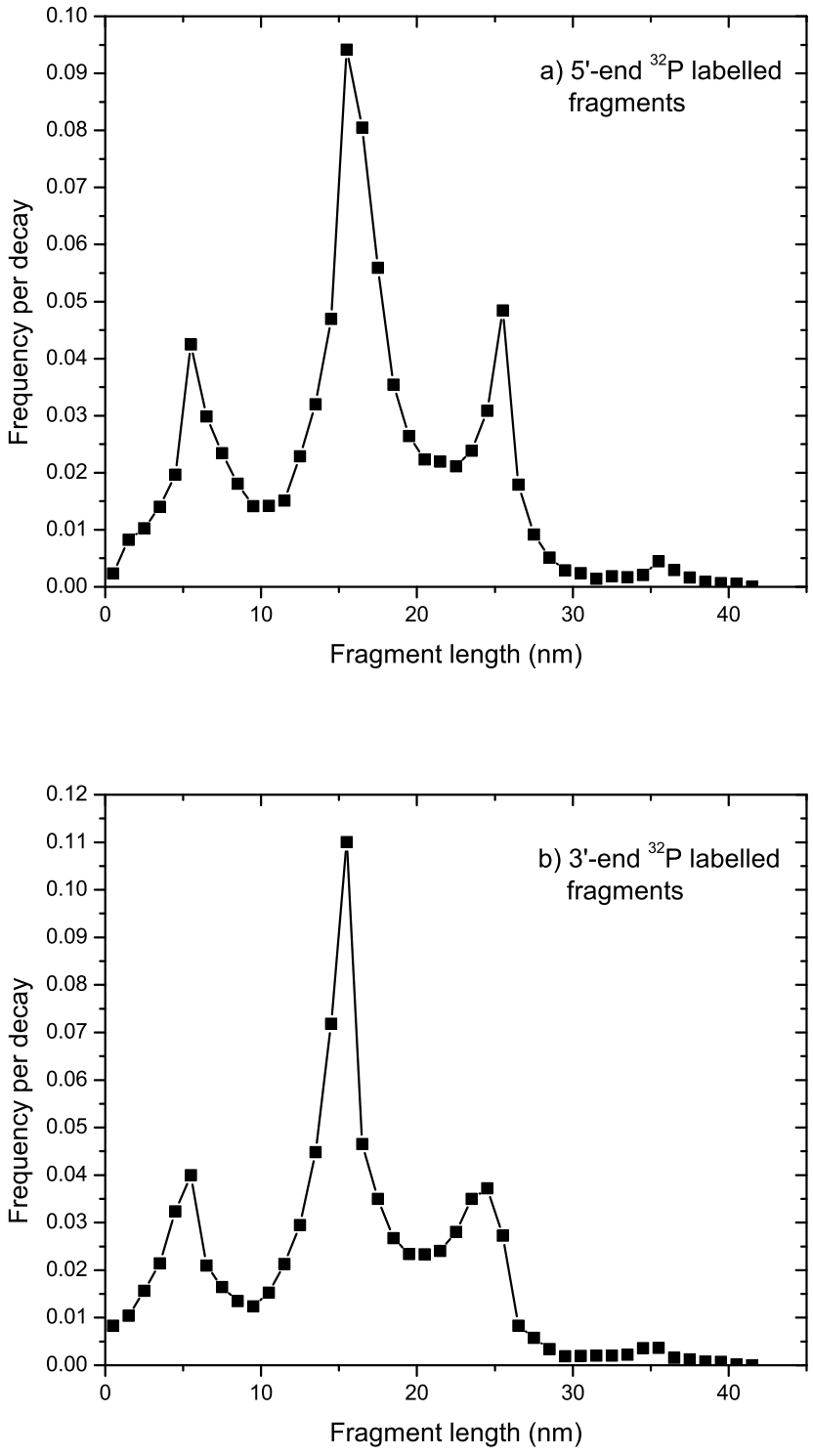

Figure 3.9: The fragment size distribution resulting from breakage in the bottom strand. Panel a: 5′-end ^{32}P-labelled fragments; panel b: 3′-end ^{32}P-labelled fragments.

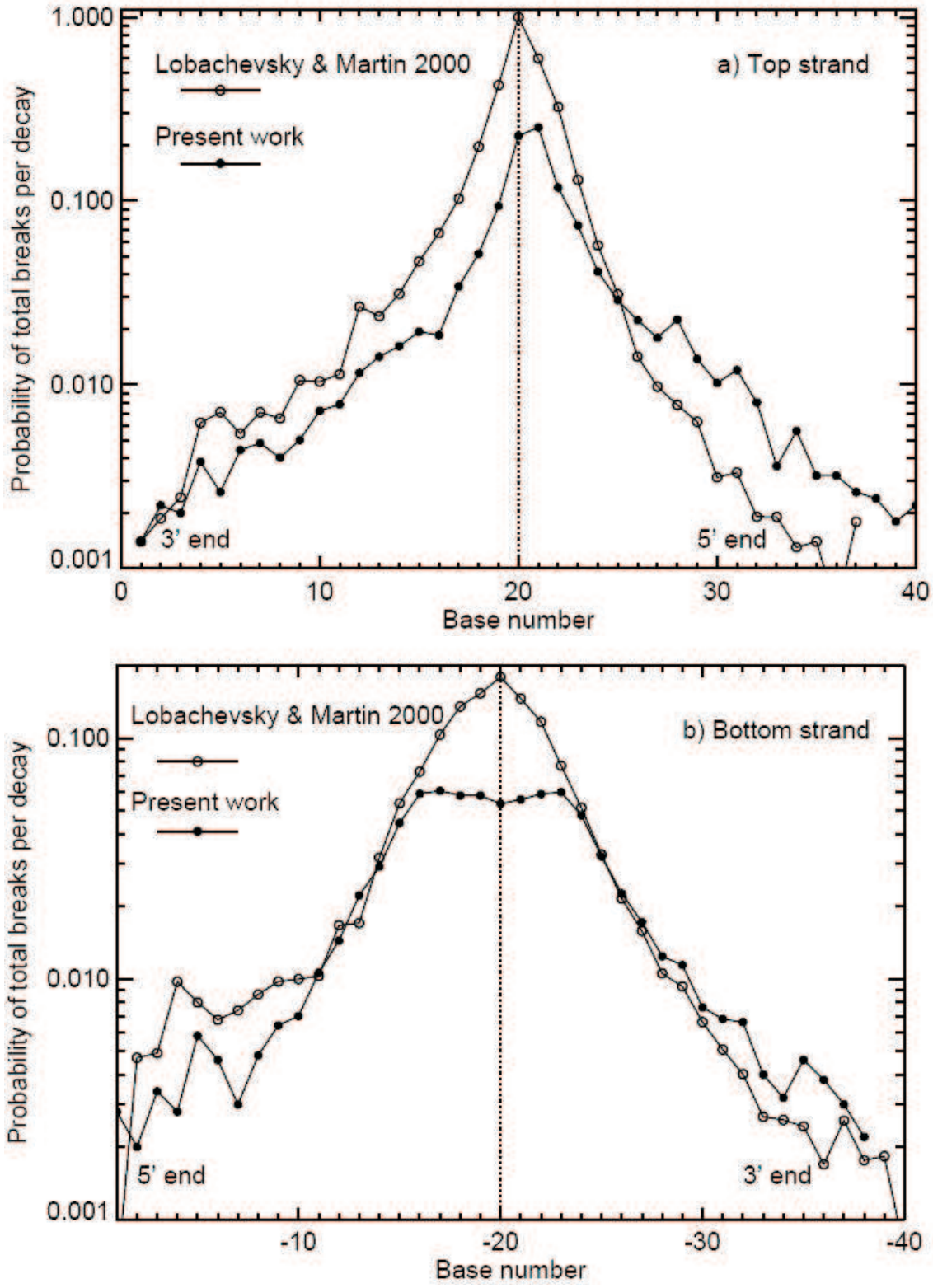

Figure 3.10: Probability of strand breaks arising from direct hits per ^{125}I decay in 41-mer oligonucleotide. The calculated results of Li [2], obtained in 2002 and results of experiment performed in PB solution with a strong scavenger by Lobachevsky and Martin [4], are shown. Panel a) shows the results for the "top", panel b) for the "bottom" strand

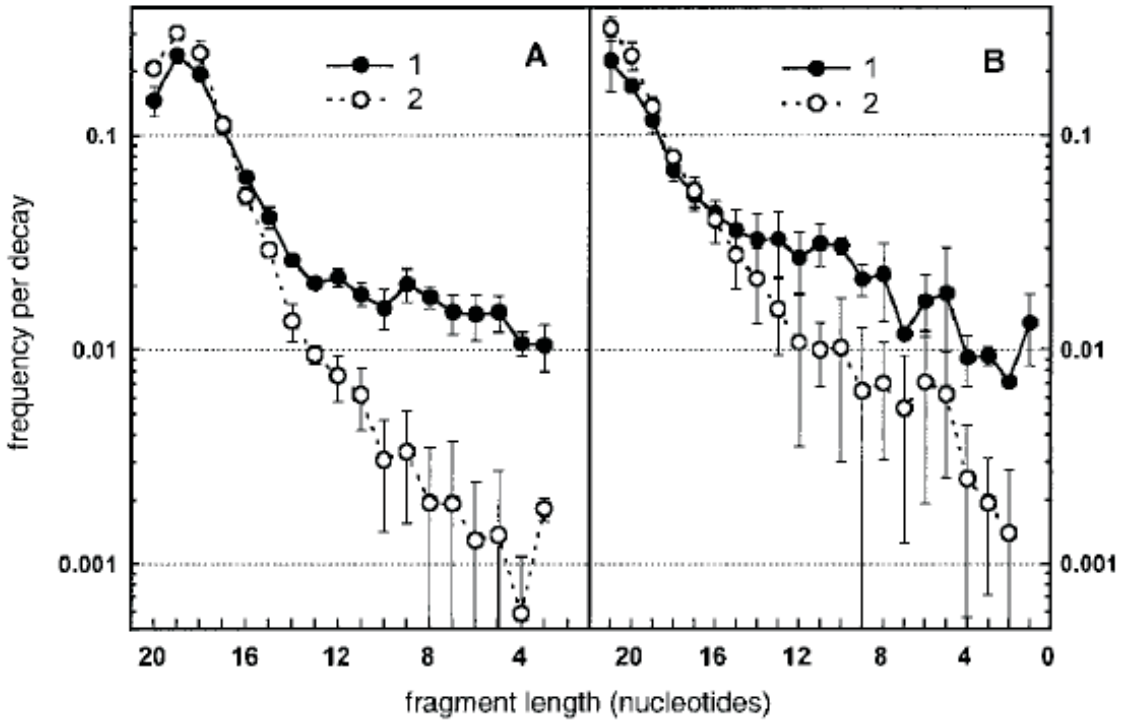

Figure 3.11: The fragment size distribution resulting from breakage in the top strand as measured by Lobachevsky and Martin [4]. Panel A: 5′-end ^{32}P-labelled fragments; panel B: 3′-end ^{32}P-labelled fragments. The line (2) shows the fragments arising from direct and quasi-direct hits (the experiment was performed in a presence of a strong scavenger), whereas the line (1) includes the action of chemical radicals (without the scavenger).

Chapter 4

Theory of Neutralization Effect

During the first Auger cascade on average 13 electrons are emitted from the Iodine atom, thus quite a high charge clearly appears on the cytosine site where the decaying atom is incorporated. As was mentioned above we assume, that this charge is quickly (in 10^{-15}s) redistributed over the DNA molecule. This means that the weakly bonded π-stack electrons of the DNA chain are transferred to the decay site. It was shown that this transfer causes additional serious damage to the DNA molecule. The purpose of this work is to estimate the extent of the damage caused by this effect. As a first method of finding this damage I've chosen the MC simulation, which is described in detail in the first part of this work, and as a second method the theoretical calculations.

Despite the charge transfer over the large molecular systems and particulary over DNA is a rapidly developing research area, the theory have not been completely developed yet. There are still a lot of unknowns though and I will explain these later.

4.1 The Fate of ^{125}I-Incorporated Molecule

One of the crucial questions is the fate of the cytosine with incorporated ^{125}I. In the past several theories have appeared, always with the same conclusion of molecule fragmentation. But as has been shown in the experiments, the cytosine can escape the fragmentation to a large extent due to the fast electron transport. Nevertheless, it was shown that the cytosine-Te bond doesn't survive the first Auger cascade.

The several semi-empirical quantum mechanics calculations were performed to calculate the molecular configuration after the Iodine decay ([2], [7]). The last was done by Pomplun ([7]) with the `HyperChem` program system. In this calculation

model, the iodine and then tellurium were attached on the C5 atom. Subsequently, the charge on the molecule was increased in steps of one unit.

The results of the calculations were characterized by the bond lengths between the iodine:tellurium atom and the C5 atom. As long as the charge is below +5 there are only small alterations. At +5, the bond length increases by more than 20% compared with the +4 state. At +6 the calculations no longer converge and a stable structure does not seem to be possible. This probably means that the second cascade induced by the internal conversion after the decay of the metastable Te state would take place when the atom is no longer part of the molecule and may have been moved away from the original position. However the $^{125m}\mathrm{Te}^{+n}$ ion probably stays in close neighborhood of original decay site.

4.2 Charge Transfer Theory

Double stranded deoxyribonucleic acid (DNA) represents a well-characterized system containing an extended π stack within its interior (Figure 4.1). This π stack represents a unique medium for electron transfer.

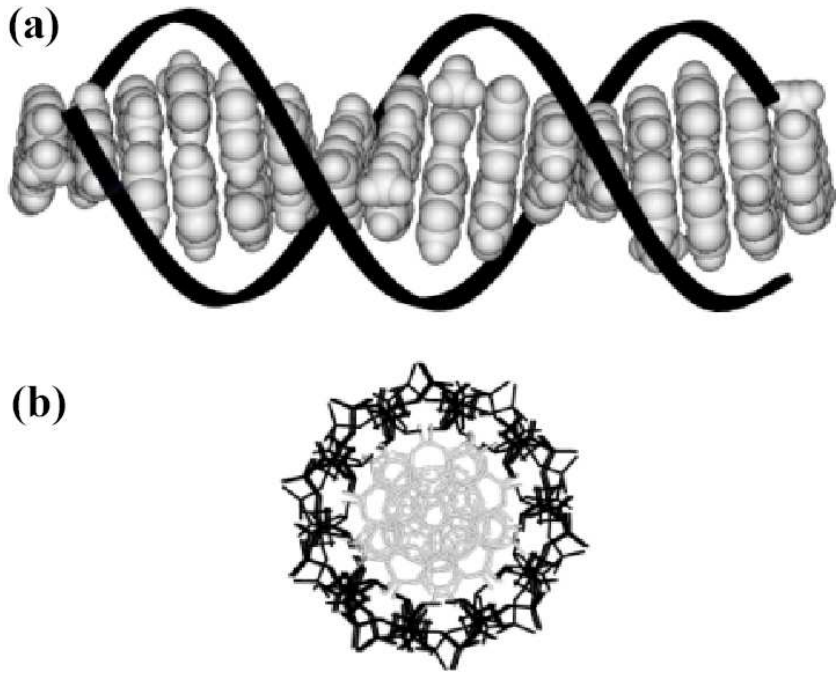

Figure 4.1: Views of B-form DNA perpendicular to (a) and down (b) the helical axis of Π-stacked bases. Taken from [23].

The process that follows the decay can be described as a hole transfer from a hole donor (Te ion) to a hole acceptor (a nucleobase) or as a transfer of electron from an electron donor (a nucleobase) to an acceptor (Te). Obviously, these two descriptions are equivalent, so I've chosen the second variant that is typically theoretically described in literature. However experiments mostly deal with a hole (positive charge) transfer as will be shown later.

The simplest case of electron transfer (ET) can be characterized by the following scheme:

$$D^- A \rightarrow D A^- \tag{4.1}$$

where D is an electron donor and A an acceptor. However in our case the problem is a bit more complicated. The donor and acceptor units are mostly not neighbors. The transport is thus mediated by some bases that bridge the donor and the acceptor. The transport is often called *bridge assisted* or *bridge mediated* and the sequence often called a donor-bridge-acceptor (DBA) system. This means we have to consider a charge migration in a system $DB_1B_2 \ldots B_{N_B}$A, where $B_j, j = 1, .., N_B$ are the N_B nucleobases of the bridge, which may belong to both strands of DNA. The electronic states are denoted by wave functions describing localized states

$$|D\rangle = |DB_1B_2 \ldots B_{N_B}A\rangle \tag{4.2}$$

$$|A^{\pm}\rangle = |D^{\mp}B_1B_2 \ldots B_{N_B}A_{\pm}\rangle \tag{4.3}$$

$$|B_j^{\pm}\rangle = |D^{\mp}B_1B_2 \ldots B_j^{\pm} \ldots B_{N_B}A\rangle \tag{4.4}$$

The superscripts + and - refer to hole and electron transfer, respectively.

The next sections will deal with the electron transfer theory and describe some of the previous and present efforts aimed at understanding the migration of charge through the DNA double helix.

4.2.1 The Electron Transfer Hamiltonian

Although ET comes along with the modification of many molecular orbits, and thus has to be considered as a process in which different electrons take part, it is possible to proceed with a simple and intuitive picture. It is based on the notion of a single *excess* electron injected from outside into a DBA complex. The transfer of this electron is described by introducing an effective potential experienced by the excess electron after entering the DBA complex

$$V(\mathbf{r}) = \sum_m V_m(\mathbf{r}) \tag{4.5}$$

The individual contributions $V_m(\mathbf{r})$ belong to the donor, the acceptor, or to the N_B bridging units.

The introduction of the effective potential $V(\mathbf{r})$ appears to be reasonable even though there is no unique way of separating it into the various $V_m(\mathbf{r})$. Each of these contributions $V_m(\mathbf{r})$ can be understood as a so-called *pseudo-potential*, which mimics the action of the total electronic system of the m-th nucleobase on the excess electron. So all the exchange and correlation effects among the excess electron and the electrons of the molecule are replaced by a simple single particle potential, which is local in space. The various V_m are defined by demanding their ground state E_m should coincide with the electronic ground state *plus* the excess electron.

The pseudo potential V_m enters the single electron Schrödinger equation which determines the single-particle energies E_m and wave functions $\varphi_m(\mathbf{r})$:

$$(T_{el} + V_m(\mathbf{r})) = E_m \varphi_m(\mathbf{r}) \tag{4.6}$$

Again, only the lowest eigenvalue E_m is of interest in the following, although higher-energetic solutions may exist. Since the energies E_m correspond to different sites in the complex, they are usually called *site energies*.

We can imagine the situation as it is sketched in Fig.4.2. The excess electron, when localized on a certain base is trapped there in a potential well (for this well we can assume a harmonic oscillator approximation) and it proceeds to the next base via a tunnelling process. Thus the final Hamiltonian of the excess electron is composed from two parts - one describing it's movement in a potential well (harmonic oscillator) and the second describing it's coupling with the other bases

$$H_{DBA} = \sum_{m,n} \{\delta_{mn} H_m(q) + (1 - \delta_{mn}) V_{mn}\} |\varphi_m\rangle\langle\varphi_n| \tag{4.7}$$

where

$$H_m(q) = U_m^{(0)} + \frac{1}{2} \sum_{\xi} \{p_\xi^2 + \omega_{m,\xi}^2 (q_\xi - q_\xi^{(m)})^2\} \tag{4.8}$$

and

$$V_{mn} = \frac{1}{2} \langle\varphi_n | V_m + V_n | \varphi_m\rangle \tag{4.9}$$

q_ξ are normal mode coordinates, $U_m^{(0)}$ and $q_\xi^{(m)}$ define the energy coordinate of stationary point as shown on Fig.4.2. And The precise derivation can be found in [24].

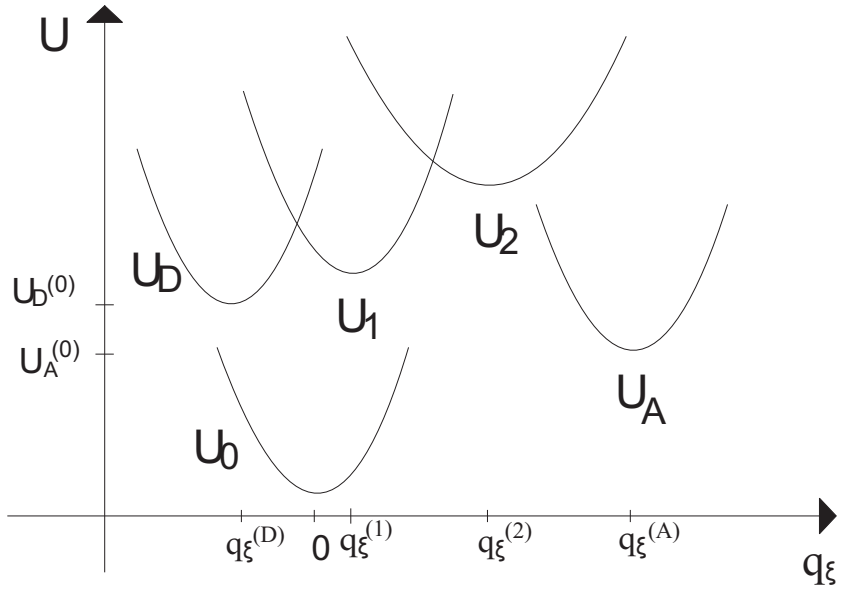

Figure 4.2: Potential energy surfaces (PES) of DA complex versus a single normal mode coordinate q_ξ. U_0 is the reference PES of the neutral complex, the PES U_m correspond to the situation where on excess electron is present at the donor (m = D), the acceptor (m = A) or at the bridge unit (m =1,2).

4.2.2 The Golden Rule of Quantum Mechanics

The motion of the electron/hole can be then described by time dependent occupation probabilities $P_a(t)$ of certain quantum systems $|a\rangle$ defined above. The P_a are obtained as the solutions of a rate equation of the type

$$\frac{\partial}{\partial t}P_a = -\sum_b (k_{ab}P_a - k_{ba}P_b) \tag{4.10}$$

where k_{ab} are transfer or transition rates. They define the probability of transition from state $|a\rangle$ to state $|b\rangle$ per time unit. This equation was at first "intuitively derived" by W. Pauli in 1928 and is usually called the *Master equation*.

The transition rate for the superexchange, bridge mediated transfer can be derived using the *Fermi's Golden Rule* (alternatives can be found e.g. in [24]). It gives us

$$k_{ET} = \frac{2\pi}{\hbar}|V_{DA}^{(eff)}|^2\mathcal{D}(\Delta E) \tag{4.11}$$

$V_{DA}^{(eff)}$ is already mentioned effective DA transfer integral and I will discuss it in detail later. $\mathcal{D}(\Delta E)$ is a combined density of states, in this context often called the *Frank-Condon factor* and denoted F. If we make an approximation for high-temperature i.e. if the relation $k_BT >> \hbar\omega_\xi$ holds for all vibrational modes ξ,

$\mathcal{D}(\Delta E)$ can be calculated. It then reads

$$\mathcal{D}(\Delta E) = \frac{1}{\sqrt{4\pi k_B T E_\lambda}} \exp\{-\frac{(\Delta E - \lambda)^2}{4\lambda k_B T}\} \tag{4.12}$$

ΔE is an energy gap between the donor and acceptor, i.e. $U_D^{(0)} - U_A^{(0)}$ (see Fig.4.2). λ is called *reorganization energy*. It is an energy needed to reorganize nuclear configuration when the hole passes from the donor to the acceptor.

4.2.3 Bridge-Assisted Electron Transfer

Since now I will focus on the hole transfer as the most experimental data are available for this kind of transport. It has been concluded from them as well as from theory that hole transfer occurs as a hopping between guanine (G) bases, that is, the nucleobases with the lowest oxidation potential *in vitro* ([25]). They further show that GG and GGG doublets/triplets act as shallow hole traps in DNA ([26]).

For hole transport via G groups, hopping may involve intrastrand as well as interstrand individual hopping steps ("zigzagging"), occurring between G bases on different strands, which belong to neighboring Watson-Crick pairs. For example in the duplex

$$\begin{array}{ccccccccccc} G_1^+ & & & G_2 & & C & & & C & & G_5 \\ | & (\text{T-A})_n & | & \ddots & | & (\text{T-A})_{n'} & | & \ddots & | & \ldots \\ C & & & C & & G_3 & & & G_4 & & C \end{array}$$

the pairs G_2, G_3 and G_4, G_5 correspond to interstrand coupling, whereas intrastrand occurs for the pairs G_1, G_2 and G_3, G_4.

The mechanism of hole transport in a duplex $DG_1(T–A)_nG_2...G_1A$ containing N guanine nucleobases separated by $(T–A)_n$ bridges between a donor and acceptor, e.g., G, GG or GGG, involves several steps:

(i) hole injection from D to the proximal G_1

(ii) a sequence of hole hopping processes between adjacent guanines, i.e., G_j and G_{j+1} within the bridge;

(iii) termination by hole trapping/detrapping between G_N and A.

The individual hole hopping processes (ii) between G_j and G_{j+1} fall into two categories - superexchange mediated hopping and thermally induced hopping.

4.2.3.1 Superexchange Mediated Hopping

. This mechanism takes place when the $(T–A)_n$ is moderately short (n≤4). It is induced by off-resonance electronic coupling between G_j and G_{j+1} via the $(T–A)_n$ subbridges. The subbridge units support a delocalization of the donor (G_j) state wave function (Fig.4.3). This delocalization essentially modifies the (electronic) coupling between the donor (G_j) and acceptor (G_{j+1}) which can be expressed by introducing an *effective* DA transfer integral. This mechanism is characterized by an exponential D-A distance dependence. The hole states of the $(T–A)_n$ subbridge are virtual and do not constitute a real chemical intermediate. The kinetic scheme for the individual unistep superexchange hopping rate is

$$G^+(T-A)_nG \overset{k_{super}}{\longrightarrow} G(T-A)_nG^+ \tag{4.13}$$

This physical picture of unistep hole superexchange between guanines separated by 'short' $(T–A)_n$ (n≤4) subbridges was proposed and analyzed in detail e.g. in [24], [27], [28], [29].

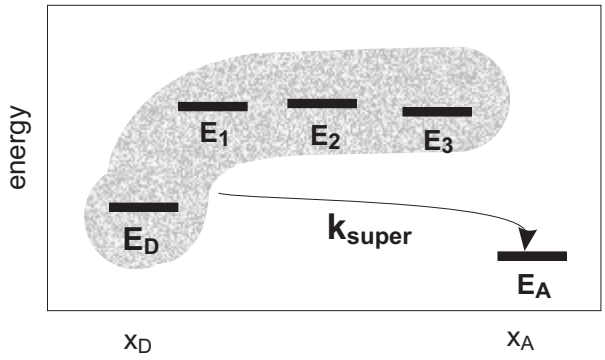

Figure 4.3: Superexchange mechanism of bridge-mediated ET between a donor and an acceptor connected by a chain of 3 bridging units (1,2,3). The bridge levels are energetically well separated from the donor and acceptor levels and the initial wave function (shaded area) extends over the whole bridge.

And now, let me derive the effective transfer integral $V_{DA}^{(eff)}$. At first let's watch the simplest case of a single bridge unit. The delocalization of the donor wave function induced by the bridge can be estimated by perturbation theory. The lowest-order correction to the donor state $|D\rangle$ following from the coupling to the bridge is given by

$$\delta|D\rangle = \frac{V_{DB}^{\star}}{E_D - E_B}|B\rangle \tag{4.14}$$

For Eq.4.11 we need the square of the effective coupling matrix $V_{DA}^{(eff)}$ between modified donor state $|D\rangle + \delta|D\rangle$ and the acceptor state $|A\rangle$. The coupling obtained is

$$V_{DA}^{(eff)} = (\langle D| + \frac{V_{DB}}{E_D - E_B}\langle B|) \times V_{BA}|B\rangle\langle A| \times |A\rangle = \frac{V_{DB}V_{BA}}{E_D - E_B} \tag{4.15}$$

Now we can proceed to long bridges. At first we assume that the state $|D...N_B - 1\rangle$ is known, where the electron is delocalized across all bridge units except the last one. Then, an effective donor-acceptor coupling $V_{DA}^{(eff)}$ is obtained in a way analogical to Eq.4.15

$$V_{DA}^{(eff)} = \frac{V_{D,N_B}^{(eff)}V_{N_B,A}}{E_D - E_{N_B}} \tag{4.16}$$

The formula contains the effective coupling $V_{D,N_B}^{(eff)}$ between the state $|D...N_B - 1\rangle$ where the electron is delocalized up to the bridge unit $N_B - 1$, and the last unit N_B of the bridge. To determine $V_{D,N_B}^{(eff)}$ we introduce the similar effective coupling $V_{D,N_B-1}^{(eff)}$ which now describes the interaction between the state $|D...N_B - 2\rangle$, where the electron is delocalized up to the bridge unit $N_B - 2$, and the bridge unit $N_B - 1$. We obtain

$$V_{DN_B}^{(eff)} = \frac{V_{D,N_B-1}^{(eff)}V_{N_B-1,N_B}}{E_D - E_{N_B-1}} \tag{4.17}$$

In the same way we may compute $V_{D,N_B-1}^{(eff)}$. If this procedure is repeated until the donor level is reached the effective donor acceptor coupling follows as

$$V_{DA}^{(eff)} = \frac{V_{D1}}{E_D - E_1}\frac{V_{12}}{E_D - E_2}\cdots\frac{V_{N_B-1,N_B}}{E_D - E_{N_B}}V_{N_B,A} \tag{4.18}$$

Recently Voityuk *et al.* ([28], [27]) have calculated electronic coupling elements $V_{B_1B_2}$ for a hole transfer between individual bases B_1 and B_2 by quantum mechanical model systems. Concretely, all possible pairs for intrastrand and interstrand combinations always in both directions ($3' \to 5'$ and $5' \to 3'$) were calculated using two-state model (for a description of the model see [30]). Using the same notation I denote intrastrand nucleobases 5′–B_1–B_2–3′ as B_1–B_2 ; the base of the opposite strand complementary to B_i will be referred as b_i (see Fig.4.4). Similarly I will denote the two different configurations of interstrand pairs 5'–B_1–b_2–5' and 3'–B_2–b_1–3' as $B_1\backslash\ b_2$ and B_2/b_1, respectively. The values for the electronic coupling matrix elements are shown in Table 4.1.

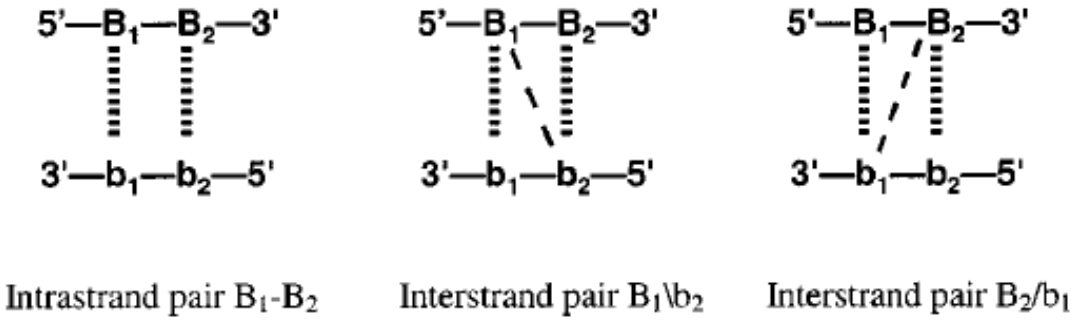

Figure 4.4: A scheme of base pairs notation. Taken from [27].

	Intrastrand		Intrastrand	
Base Pair	5′ -B_1-B_2–3′	3-′ B_1–B_2-5′	B_1\ b_2	B_2/b_1
GG	0.084	0.084	0.019	0.043
AA	0.030	0.030	0.034	0.062
CC	0.041	0.041	0.0007	0.002
TT	0.158	0.158	0.003	0.001
GA	0.089	0.049	0.021	0.004
GC	0.110	0.042	0.010	0.025
GT	0.137	0.085	0.009	0.013
AC	0.061	0.029	0.001	0.013
AT	0.105	0.086	0.016	0.007
CT	0.100	0.076	0.001	0.003

Table 4.1: Electronic coupling matrix elements (in eV) for hole-transfer between two nucleobases in the regular structure of DNA calculated using two-state model

The transfer rates further depends on the value of the reorganization energy λ and the energy gaps between the donor and the bridge units and the donor and the acceptor. In the case of a DNA oligomer in a solution, the reorganization energy is divided by two parts - the solvent and internal (molecular) reorganization energy. Often, the solvent component is treated classically, whereas the internal component is calculated with a quantum chemical approach ([31]). The values for λ and ΔE were estimated by calculations ([31]) and finally chosen to obtain the best agreement with experiments ([29]. The values for λ were considered to be similar for all the sequences and to depend only on the length of the bridge. This gives

the values $\lambda_1 = 0.3$ eV, $\lambda_2 = 0.4$ eV, $\lambda_3 = 0.62$ eV, Δ G = -0.7 eV where λ_1, λ_2, λ_3 correspond to the values of reorganization energy for one, two and three AT base pairs in a bridge, respectively.

The energy gaps were measured empirically and read: $\Delta E(G-A) = 0.22 \pm 0.05$ eV, $\Delta E(G-T) = 0.6$ eV and $\Delta E(G-C) = 0.6$ eV. Further ΔE, the energy gap between the neighboring effective guanine sites (see fig.4.5) reads ΔE = 0 for symmetric $G^+ \ldots$G hole shift and ΔE=0.096 eV for hole trapping in $G^+(A-T)_n$ GGG [32].

4.2.3.2 Thermally Induced Hopping (TIH).

This mechanism prevails in 'long' $(T–A)_n$ (n≥4) bridges, which separate G_j and G_{j+1} nucleobases. Hole transport via TIH within the subbridge occurs via thermally induced donor–bridge hole excitation from G^+ to A in $(T–A)^{(1)+}$ (rate k_1), followed by hole hopping between nearest-neighbor A nucleobases (see Fig.4.5)

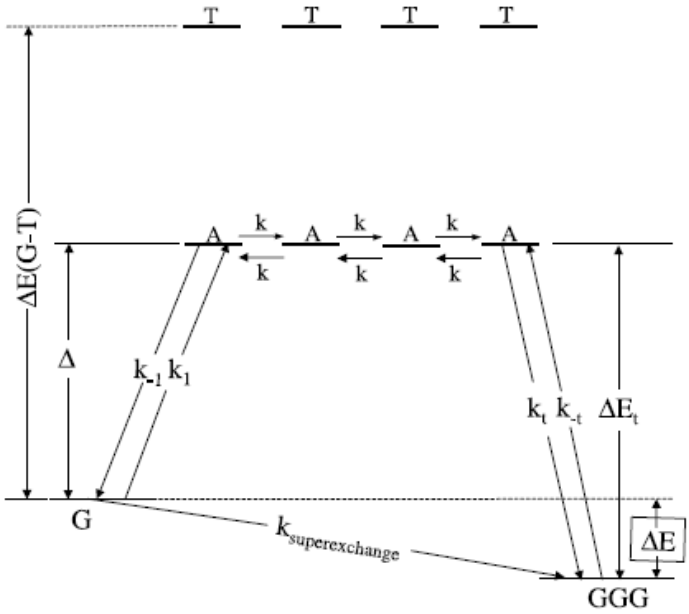

Figure 4.5: A kinetic–energetic scheme for the parallel superexchange–TIH mechanism of hole transport in G$(T–A)_n$GGG duplexes. Horizontal lines depict energy levels of the hole states. The initial/final levels correspond to G/GGG, the adenine A levels are accessible by TIH (for large n) and can also act as superexchange mediators (for small n). The thymine T levels act as superexchange mediators. The energy gaps, Δ (for G^+, ΔE (for $G^+ \ldots$(GGG)), ΔE_t (for A^+(GGG)) and ΔE(G–T) (for G-T), are marked on the figure. The arrows represent individual rates for charge injection (k_1), recombination (k_{-1}), hopping (k), and trapping/detrapping (k_t, k_t). k_{super} denotes the unistep superexchange rate.

within the bridge (hopping rates k) and being terminated by hole trapping (rate k_t). The calculations also have to include hole deexcitation (rate k_{-1}) and hole detrapping (rate k_{-t}) from/to the adenines bridge.

The rate k_{TIH} of hole transfer between the neighboring effective guaninens is given by

$$k_{TIH} = k \exp(-\Delta/k_B T)/[(k/k_{-1}) + (k/k_t) + (n-1)] \tag{4.19}$$

where $\Delta(>0)$ is the energy gap between $G^+(T-A)^{(1)}$ and $G(T-A^+)^{(1)}$ (c.f. Fig.4.5). It was estimated as $\Delta = 0.22 \pm 0.05eV$ [32].

The superexchange and TIH are competing mechanisms. As was said the superexchange is more successful for short bridges. For the bridge length 3-4, the transition rates for both mechanisms are approximately equal (see Fig.4.6).

In our studied structure (c.f. Fig.3.4), there is just one place where we could consider the TIH. There the distance between guanines is 4 nucleobases. But

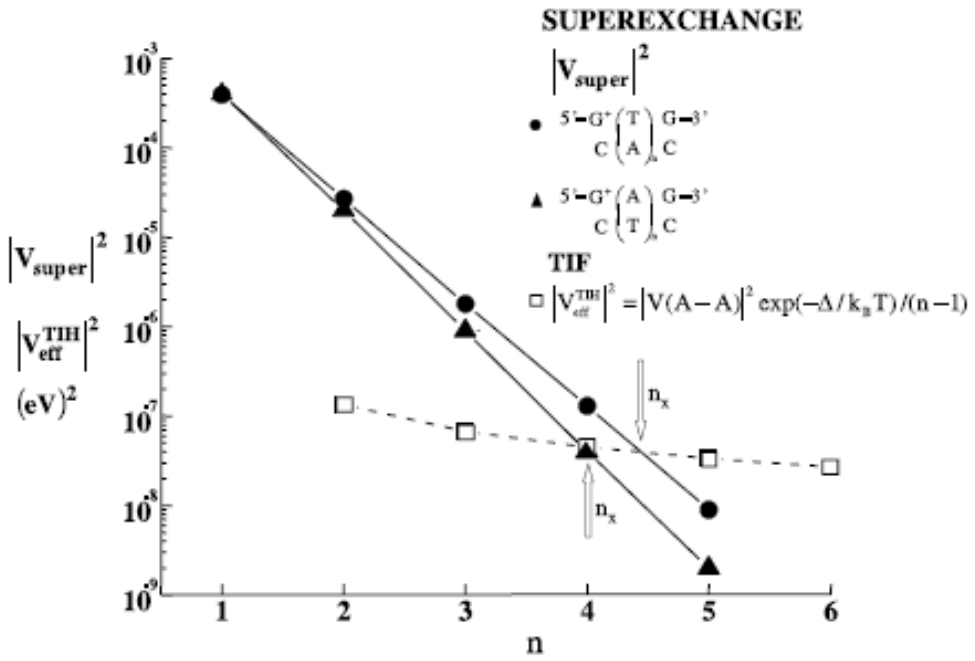

Figure 4.6: A quantum mechanical description of the crossover from superexchange to TIH in $G^+(T–A)_nG$ duplexes with increasing the bridge size. The solid lines with closed circles and triangles represent $|V_{super}|^2$ for the two duplexes marked on the figure. The dashed line with open squares represents $|V_{eff}^{TIH}|^2$ with Δ=0.22 eV. The 'critical' size values, n_x, are marked by vertical arrows.

according to Fig.4.6 for such a distance the transition rates of both mechanisms are approximately equal. Thus I would assume just superexchange mediated charge hopping in a whole structure.

Consequently we have all the necessary data to perform a calculation of the probability of charge transfer in our model system that would help to understand the process following the radiation. As it is again a stochastic process the Monte Carlo method would be an appropriate tool. Unfortunately there are still a lot of questions concerning the applicability of the model described above. The main questions are following:

- This model was derived for a single charge travelling through the chain, but in our case there are in average 13 holes initially present on Te ion. Can we assume that the electrons transfer separately one after another? Otherwise the energy transferred exceeds much the chemical bond energy. What happens in this case?
- What kind of damage do the extracted electrons actually cause?
- Is the model of hopping under guanines still applicable if there are already holes present on them? The same holds for the typical trap of guanines triplet - does it still work like a trap if there is already one or more holes present on it?

Chapter 5

Conclusions and further perspectives

In the present study a new model for the radiation action of ^{125}I incorporated in the DNA is introduced. This model is needed for several reasons. This radioisotope is widely used in nuclear medicine. For the detailed understanding of toxic effect of Iodine, the good prediction of the DNA damage is necessary. Experiments have also shown that the Iodine decay can be used for determining DNA conformations that are otherwise difficult to recognize with other experimental methods.

The model has not been completed yet. The process following the decay can be divided into 3 phases:

- the physical phase including the direct interaction of the radiation with DNA molecule and its water shell,
- the chemical phase including the interaction of the radiation with a bulk water, creation of chemical radicals and its migration towards DNA,
- the neutralization effect.

So far, the part of the model simulating the physical phase has been written, tested and applied. The results, with its comparison to the experimental data and to previous simulations are presented and discussed in the section 3.3. The results obtained with presented model do not agree well with the ones published by other authors. From the analysis we conclude that the part responsible for the discrepancy is the part simulating the energy spectrum of Auger electrons. The part of the program based on the results of Pomplun [11] results has to be improved to achieve a good agreement for the direct and quasi-direct effect of the decay. Afterwards the

whole program will be extended to also include the chemical phase and eventually also the neutralization effect.

The second part of the work (c.f. section 4) was devoted to the theory of neutralization effect. This theory is developing fast nowadays and gives more and more precise information about the charge transfer. Lot of knowledge missing though, especially concerning the transfer of more electrons. An attempt to use the presented theoretical results in a simulation of ^{125}I decay can help to understand the multiple electron transfer as well as what is happening inside the DNA after the decay.

Bibliography

[1] Panyutin IG and Neumann RD. Sequence-specific DNA double-strand breaks induced by triplex forming ^{125}I labelled oligonucleotides. *Nucleic Acids Res.*, 22(23):4979–4982, 1994.

[2] Weibo Li. *Iodine-125 induced DNA strand breakage: Contribution of different physical and chemical radiation action mechanism.* PhD thesis, Tehnische Universität München, 2002.

[3] Booz J, Charlton DE and Pomplun E. X-ray induction of the Auger effect: Quantification of the different energy transfer mechanisms and dosimetric implications. In *Proceedings of the eight symposium on Microdosimetry*, pages 611–624. Comission of the European Communities, Luxembourg, 1982.

[4] Lobachevsky PN and RF Martin. Iodine-125 decay in a synthetic oligodeoxynucleotide. I. Fragment size distribution and evaluation of breakage probability. *Radiat. Res.*, 153:263–270, 2000.

[5] Martin RF and Lobachevsky PN. Iodine-125 decay in a synthetic oligodeoxynucleotide. II. The role of Auger electron irradiation compared to charge neutralization in DNA breakage. *Radiat. Res.*, 153:271–278, 2000.

[6] Martin RF, Lobachevsky PN, Karagiannis TC. Plasmid DNA breakage by decay of DNA-associated Auger electron emitters: Approaches to analysis of experimental data. *Radiat. Res.*, 162:84–95, 2004.

[7] Pomplun E. The basic data for understanding the Auger effect. *Acta Oncologica*, 39(6):673–679, 2000.

[8] Charlton DE and Booz J. A Monte Carlo treatement of the decay of ^{125}I. *Radiat. Res.*, 87:10–23, 1981.

[9] Booz J, Pomplun E and Charlton DE. A Monte Carlo simulation of Auger cascades. *Radiat. Res.*, 111:533–552, 1987.

[10] Pomplun E. A new DNA target model for track structure calculations and its first application to I-125 auger electrons. *Int. J. Radiat. Biol.*, 59(3):625–642, 1991.

[11] Pomplun E and Sutmann G. Is coulomb explosion a damaging mechanism for $^{125}IUDR$. *Int. J. Radiat. Biol.*, 80:855–860, 2004.

[12] Pomplun E and Terrissol M. Low-energy electrons inside active DNA models - a tool to elucidate the radiation action mechanisms. *Radiat. Environ. Biophys.*, 33:279–292, 1994.

[13] Terrissol M, Vrigneaud JM, Nikjoo H, Panyutin IG and Laughton CA. Distribution of strand breaks produced by Auger electrons in decay of ^{125}I in triplex DNA. *Acta Oncologica*, 39(6):707–712, 2000.

[14] Paretzke HG Stork T Friedland W, Jacob P. Monte Carlo simulation of the production of short DNA fragments by low-linear energy transfer radiation using higher-order DNA models. *Radiat. Res.*, 150(2):170–182, 1998.

[15] Paretzke HG, Friedland W, Jacob P et al.. Simulation of DNA fragment distributions after irradiation with photons. *Radiat. Environ. Biophys.*, 38(1):39–47, 1999.

[16] Jacob P *et al.* Li WB, Friedland W. Simulation of I-125 decay in a synthetic oligodeoxynucleotide with normal and distorted geometry and the role of radiation and non-radiation actions. *Radiat. Environ. Biophys.*, 43(1):23–33, 2004.

[17] Alberts B *et al.*. *Molecular Biology of The Cell.* Garland Science, 4th edition, 2002.

[18] Bigildeev EA and Michalik V. Charged particle tracks in water of different phases. Monte Carlo simulation of electron tracks. *Radiat. Phys. Chem.*, 47(2):197–207, 1996.

[19] Bigildeev EA, Burmistrov DS, Lappa AV and Vasilyev ON. `Trion` code for radiation action calculations and its application in microdosimetry and radiobiology *Radiat. Environ. Biophys.*, 32(1):1–19, 1993.

[20] Martin RF and Lobachevsky PN. DNA strand breakage by I-125-decay in a synthetic oligodeoxynucleotide. Quantitative analysis of fragment distribution. *Acta Oncologica*, 35(7):809–815, 1996.

[21] Merz KM, Stanton RV, Cheng AL, Vincent JJ, Crowley M, Tsui V, Gohlke H, Radmer RJ, Duan Y, Pitera J, Massova I, Seibel GL, Singh UC, Weiner PK, Simmerling, Darden TA and Kollman PA. *AMBER 7*. University of California, San Francisco, 2002.

[22] Begusova M. DNA radiolysis. Experimental study and theoretical modeling of the effects of DNA structure and ligands. PhD thesis, Tehnische Université d'Orléance, 1999.

[23] Treadway CR, Hill MG, Barton JK. *Introduction to Charge Transfer and Charge Transport Through the DNA Double Helix.* Chem. Phys. 281:409–428, 2002.

[24] May V and Kühn O. *Charge and Energy Transfer Dynamics in Molecular Systems, 2nd, Revised and Enlarged Edition.* Wiley-VCH, Berlin, 2003.

[25] Yan M, Sevilla MD, Becker D and Summerfield SR. Relative abundances of primary ion radicals in γ-irradiated DNA: Cytosine vs Thymine anions and Guanine vs Adenine Cations. *J. Phys. Chem.*, 95:3409–3415, 1991.

[26] Barton JK, Williams TT, Odom DT. Variations in DNA charge transport with nucleotide composition and sequence. *Journal Of The American Chemical Society*, 122:9048–9049, 2000.

[27] Bixon M, Voityuk AA and Jortner J. Electronic coupling between Watson-Crick pairs for hole transfer and transport in desoxyribonucleic acid. *J. Chem. Phys.*, 114:5614–5620, 2001.

[28] Bixon M, Jortner J, Voityuk AA and Roesch N. Electronic coupling for charge transfer and trnasport in DNA. *J. Phys. Chem. B*, 104:9740–9745, 2000.

[29] Pettitt MB, Lakhno VD and Sultanov VB. Combined hopping-superexchange model of a hole transfer in DNA. *Chem. Phys. Letters*, 400:47–53, 2004.

[30] Newton MD. Quantum chemical probes of electron-transfer kinetics - the nature of donor-acceptor interactions. *Chemical Reviews*, 91(5):767–792, 1991.

[31] Newton MD, Siriwong K, Voityuk AA and Roesch N. Estimate of the reorganization energy for charge transfer in DNA. *J. Phys. Chem. B*, 107:2595–2601, 2003.

[32] Bixon M and Jortner J. Long-range and very long-range charge transport in DNA. *Chem. Phys.*, 281:393–408, 2002.